

ATMOSPHERIC NEUTRINOS *

E.Kh. Akhmedov †

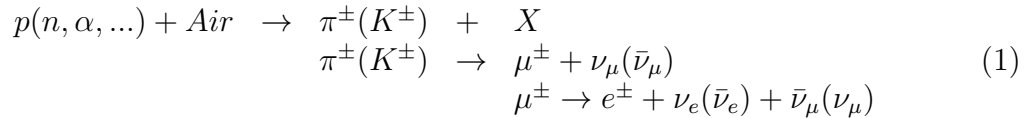
Instituto de Fisica Corpuscular (IFIC-CSIC)
Departamento de Fisica Teorica
Universitat de Valencia
c/ Dr. Moliner, 50
46100 Burjassot (Valencia) Spain

Abstract

Recent results of atmospheric neutrino experiments are reviewed and their possible interpretations are discussed, main emphasis being put on the neutrino oscillation hypothesis.

1 Introduction

Atmospheric neutrinos provide us with a unique tool of studying neutrino properties in a wide range of neutrino energies and for vastly differing distances between the neutrino birthplace and the detector. They also constitute a background in the underground proton decay experiments. These are electron and muon neutrinos and their antineutrinos which are produced in the hadronic showers induced by primary cosmic rays in the earth's atmosphere. Their energies range from a few hundred MeV to more than 100 TeV. The main mechanism of production of the atmospheric neutrinos is given by the following chain of reactions:



Atmospheric neutrinos can be observed directly in large mass underground detectors by means of their charged-current interactions:

$$\nu_e(\bar{\nu}_e) + A \rightarrow e^-(e^+) + X \tag{2}$$

*Invited talk at the Intern. School on Cosmological Dark Matter, Valencia, Spain, October 4-8, 1993

†On leave of absence from National Research Center "Kurchatov Institute", 123182 Moscow, Russia

$$\nu_\mu(\bar{\nu}_\mu) + A \rightarrow \mu^-(\mu^+) + X \quad (3)$$

The atmospheric neutrino events can be subdivided into several groups, depending on the energy of the charged leptons produced. “Contained events” are those where the neutrino–nucleus interaction vertex is located inside the detector and all final state particles do not get out from it. These events have charged lepton energies in the range from a few hundred MeV to 1.2 GeV. Muon neutrinos can also be detected indirectly by observing the muons that they have produced in the material surrounding the detector. To reduce the background from atmospheric muons, only upward–going neutrino-induced muons are usually considered. A rough estimate of the energy spectrum of the upward–going muons has been obtained dividing them in two categories, passing (or through-going) and stopping muons. The latter, which stop inside the detector, have the energies ranging typically from 1.2 to 2.5 GeV, whereas the through-going muons have the energies $\gtrsim 2.5$ GeV.

Recently there has been a considerable interest in atmospheric neutrinos due to an anomaly observed in the contained neutrino induced events by the Kamiokande^{1,2} and IMB³ collaborations. Both groups measure the ratio of muons to electrons and find it smaller than what is predicted by several independent theoretical calculations⁴. A possible interpretation of the effect has been given in terms of $\nu_\mu \leftrightarrow \nu_x$ oscillations, where ν_x can be ν_e , ν_τ or a sterile neutrino ν_s , with typical values of the oscillation parameters $\Delta m^2 \sim 10^{-3} \div 10^{-2}$ eV² and $\sin^2 2\theta \geq 0.5$ (a summary is contained in ref.⁵). For this range of parameters, the flux of upward–going muons could also be observably reduced. However, the IMB, Baksan and Kamiokande experiments did not observe any such reduction^{6,7,8}, thus setting rather stringent limits to the allowed region in the $(\Delta m^2, \sin^2 2\theta)$ plane. In this Lecture we will discuss various aspects of the atmospheric neutrino anomaly and its possible interpretations.

2 Predicted atmospheric neutrino fluxes and the data

Contained events

Naively, from the reaction chain of Eq. 1 one would expect to have two atmospheric muon neutrinos or antineutrinos for every electron neutrino or antineutrino. In reality, this is not quite true: one should take into account the differences in the lifetimes of π^\pm , K^\pm and μ^\pm as well as the differences in their spectra. Also, although the reaction chain (1) is the dominant source of atmospheric neutrinos, it is not the only one. Accurate calculation of the atmospheric neutrino fluxes is a difficult job which includes such ingredients as spectra and chemical composition of cosmic rays (including geomagnetic effects and solar activity), cross sections of π and K production off the nuclear targets, Monte Carlo simulation of hadronic cascades in the

atmosphere and the calculation of neutrino spectra including muon polarization effects. Each step introduces some uncertainty in the calculation. Below we reproduce a table of the estimated uncertainties which we borrowed from a recent talk of Todor Stanev⁹:

<u>Contained events:</u>		<u>Upward going muons:</u>	
• cosmic ray flux	~ 10%	• cosmic ray flux	
• solar cycle modulation	~ 10%	and composition	~ 15%
• geomagnetic cutoff	~ 5%	• inclusive π spectra	~ 12%
• K/π ratio	~ 3%	• K/π ratio	~ 12%
• $\nu/\bar{\nu}$ ratio	~ 5%	• $\nu/\bar{\nu}$ ratio	~ 8%
• νN cross sections	~ 5%	• νN cross sections	~ 10%

The overall uncertainty of the calculated atmospheric neutrino fluxes is pretty large, and the total fluxes calculated by different authors differ by as much as 30%. At the same time, the ratio of the muon to electron neutrino fluxes is fairly insensitive to the above uncertainties, and all the calculations taking into account the muon polarization effect yield the ratios of muon-like to electron-like contained events which agree to better than 5%. This ratio has been measured up to now by five experimental groups. Two of them (Kamiokande and IMB) use large water Čerenkov detectors, whereas the other three detectors (Fréjus, NUSEX and Soudan 2) are iron calorimeters. Muons can be distinguished from electrons in water detectors by the rings of the Čerenkov light they produce. Another way of identifying the muon-like events is by detecting the muon decay, and the results of both identification techniques are in a very good agreement with each other. Below we summarize the results of the five experiments for the double ratio, $R \equiv \frac{(\mu/e)_{data}}{(\mu/e)_{MC}}$ in the contained events (MC stands for the Monte Carlo simulations):

Experiment	Exposure ($kt \cdot yr$)	R	
Kamiokande ¹⁰	6.18	$0.60 \pm 0.06 \pm 0.05$	(rings)
		0.61 ± 0.07	(decays)
IMB ³	7.7	$0.54 \pm 0.05 \pm 0.12$	(rings)
		0.65 ± 0.05	(decays)
Fréjus ¹¹	1.56	0.87 ± 0.21	
NUSEX ¹²	0.40	0.99 ± 0.40	
Soudan 2 ¹³	1	$0.69 \pm 0.19 \pm 0.09^{*)}$	

*) preliminary result

From this table we see that the data from the water Čerenkov detectors show too small a (μ/e) ratio as compared to the Monte Carlo simulations, and the results of Kamiokande and IMB groups are in a very good agreement. This is the essence of what is called now “the atmospheric neutrino anomaly”. At the same time, the iron calorimeters give the double

ratio R which is consistent with one. Are these two sets of data inconsistent with each other? The answer is no, since the calorimeter results have lower statistical significance and in fact are consistent with the suppressed (μ/e) ratio as well.

Now the question is, if the suppression of this ratio is a real effect, is the muon neutrino flux suppressed or the electron neutrino flux enhanced? The interpretation is calculation-dependent. Below we reproduce the comparison of the Kamiokande data for double ratio R with Monte Carlo simulations using different neutrino fluxes¹⁰:

Gaisser–Stanev:

$$\frac{(\mu/e)_{data}}{(\mu/e)_{MC}} = \frac{(191/198)}{(325/203)} = 0.60 \pm 0.06 \pm 0.05$$

Lee–Koh:

$$\frac{(\mu/e)_{data}}{(\mu/e)_{MC}} = \frac{(191/198)}{(256/157)} = 0.59 \pm 0.06 \pm 0.05$$

Honda *et al.*:

$$\frac{(\mu/e)_{data}}{(\mu/e)_{MC}} = \frac{(191/198)}{(293/179)} = 0.59 \pm 0.06 \pm 0.05$$

Bugaev–Naumov:

$$\frac{(\mu/e)_{data}}{(\mu/e)_{MC}} = \frac{(191/198)}{(214/133)} = 0.60 \pm 0.06 \pm 0.05$$

We see that although the predictions for μ -like and e -like events obtained with different fluxes differ substantially, the calculated (μ/e) ratios are very close to each other, and so the double ratios R are practically the same. From the above numbers we can see that if one uses the Gaisser–Stanev or Honda *et al.* fluxes for the interpretation of the data, one would conclude that the observed muon neutrino flux is suppressed whereas the electron neutrino flux is close to the calculated one. On the contrary, the Bugaev–Naumov flux implies that the observed electron neutrino flux is enhanced whereas that of muon neutrinos is close to the calculated one. At the same time, the Lee–Koh flux implies that both the muon neutrino flux is suppressed and the electron neutrino flux is enhanced.

Upward-going muons

Upward-going muons have been observed by several experimental groups. The results are summarized below:

Kamiokande⁸:

$$F_{\mu}(> 3 \text{ GeV}) = (2.04 \pm 0.13) \times 10^{-13} \text{ cm}^{-2}\text{s}^{-1}\text{sr}^{-1},$$

Baksan⁷:

$$F_{\mu}(> 1 \text{ GeV}) = (2.83 \pm 0.14) \times 10^{-13} \text{ cm}^{-2}\text{s}^{-1}\text{sr}^{-1},$$

IMB⁶:

$$F_{\mu}(> 2 \text{ GeV}) = (2.26 \pm 0.17) \times 10^{-13} \text{ cm}^{-2}\text{s}^{-1}\text{sr}^{-1},$$

After the correction for different thresholds, all the results agree well with each other.

Since there are no electrons in the upward-going flux, one has to compare the data directly with the calculations. The results of such a comparison for different calculated ν_μ spectra and two sets of the nucleon structure functions are presented below (muon fluxes are in the units of $10^{-13} \text{cm}^{-2} \text{s}^{-1} \text{sr}^{-1}$ and correspond to the threshold $E_\mu > 3 \text{ GeV}$)⁹:

Calculations	Muon Flux		<i>(data/calc.)</i> Kamiokande		<i>(data/calc.)</i> Baksan		<i>(data/calc.)</i> IMB	
	(a)	(b)	(a)	(b)	(a)	(b)	(a)	(b)
Agraval <i>et al.</i> ¹⁴	2.36	2.11	0.86	0.97	0.88	0.99	0.81	0.91
Butkevich <i>et al.</i> ¹⁵	2.43	2.16	0.84	0.94	0.86	0.96	0.79	0.89
Mitsui <i>et al.</i> ¹⁶	2.30	2.05	0.89	1.00	0.98	1.02	0.83	0.94
Volkova ¹⁷	2.18	1.95	0.94	1.05	0.95	1.07	0.88	0.98

Here (a) and (b) refer to the calculations with the structure functions Owens'91¹⁸ and EHLQ2¹⁹, respectively. Although there is a considerable spread in the calculations, one can conclude that the data are in a good agreement with the Monte Carlo simulations, i.e. there is no indication of the deficiency of the muon neutrinos.

The main problem in analyzing the data on upward-going muons is the significant uncertainty ($\sim 20\%$) in the calculations of the total fluxes. To cure this problem, the IMB collaboration has analyzed the ratio of stopping to passing upward-going muons. In this ratio the uncertainty related to the unknown normalization of the flux cancels, and the result is dominated by the statistical errors. The value of the ratio obtained was

$$\frac{F_s}{F_p} = 0.160 \pm 0.019,$$

in an excellent agreement with their detailed Monte Carlo calculation, 0.163 ± 0.05 .

3 Interpretation of the data

Neutrino oscillations

A possible explanation of the observed anomaly in the contained atmospheric neutrino events could be oscillations of muon neutrinos into ν_x where ν_x can be ν_e , ν_τ or a hypothetical sterile neutrino ν_s . In the former case one would observe both a deficiency of atmospheric ν_μ 's and an excess of ν_e 's, whereas in the latter two cases the result would be the deficiency of the ν_μ 's. The probability of the ν_μ oscillations in vacuum in the two-flavor approximation is

$$P(\nu_\mu \rightarrow \nu_x) = \sin^2 2\theta_{\mu x} \sin^2 \left(\frac{\Delta m^2}{4E_\nu} L \right) = \sin^2 2\theta_{\mu x} \sin^2 \left(1.27 \Delta m^2 (\text{eV}^2) \frac{L (\text{km})}{E_\nu (\text{GeV})} \right). \quad (4)$$

Here $\theta_{\mu x}$ is the relevant mixing angle, Δm^2 is the squared mass difference of the neutrino mass eigenstates, and L is the distance travelled by the neutrinos. The results on the

contained events can therefore be represented as an “allowed region” on the $\sin^2 2\theta_{\mu x} - \Delta m^2$ plane (see figs. 1 and 2 below).

The important question is: Do the results on upward-going muons, in which an un-suppressed muon neutrino flux has been observed, contradict the neutrino-oscillations hypothesis as a possible explanation of the anomaly in the contained events? The answer is no (or not necessarily), since the neutrinos in these two sets of data have different characteristic energies and also travel through different distances L . The neutrinos giving rise to the upward-going muons have bigger energies than those responsible for the contained events, therefore their oscillation lengths are larger and the oscillations may not be fully developed. This effect is partly compensated by the fact that they travel through larger distances before reaching the detector. As a result, the upward-going muon data constrain the allowed ranges of the parameters of neutrino oscillations but do not exclude this mechanism completely.

Usually the atmospheric neutrino anomaly is analyzed in terms of the $\nu_\mu \leftrightarrow \nu_\tau$ oscillations. The reason for this is that the $\nu_\mu \leftrightarrow \nu_e$ oscillations are now the most popular candidate for the solution of the solar neutrino problem (the observed deficit of solar neutrinos). This would imply that they cannot be responsible for the atmospheric neutrino anomaly since the ranges of Δm^2 required in the two cases do not overlap. However, the solar neutrino deficit can be accounted for through the $\nu_e \leftrightarrow \nu_\tau$ oscillations provided the neutrino masses obey the conditions $m_{\nu_e} \approx m_{\nu_\tau} \ll m_{\nu_\mu}$ or $m_{\nu_\mu} \ll m_{\nu_e} \approx m_{\nu_\tau}$. It should be emphasized that although many popular models of neutrino mass generation predict the neutrino mass hierarchy $m_{\nu_e} \ll m_{\nu_\mu} \ll m_{\nu_\tau}$, models with quite different hierarchies also exist. Moreover, there are absolutely no experimental indications in favour of the direct hierarchy. On top of that, the solution of the solar neutrino problem may have nothing to do with neutrino oscillations. For this reason one should consider all possible kinds of the ν_μ oscillations as possible explanations of the atmospheric neutrino anomaly.

It is well known by now that the probability of neutrino oscillations in matter can differ significantly from that in the vacuum²⁰. Therefore one should take into account the matter effects on the oscillations of neutrinos passing through the earth. As we already mentioned, the simplest possibility is that the atmospheric neutrino anomaly is due to the $\nu_\mu \leftrightarrow \nu_\tau$ oscillations. In this case, since both neutrino flavors have identical interactions with matter, the oscillations will not be affected by the presence of the matter in the earth, and the simple formula of Eq. 4 applies. If, however, the initial ν_μ oscillates to ν_e or to a sterile neutrino, ν_s , the matter effects can be relevant. The oscillation probability can then be found by numerically solving the neutrino evolution equation.

For matter effects to be significant one needs²⁰

$$\frac{\Delta m^2}{E_\nu} \lesssim \sqrt{2} G_F N_A \rho = 0.758 \times 10^{-4} \rho (\text{g cm}^{-3}) \frac{\text{eV}^2}{\text{GeV}} \quad (5)$$

Neutrinos giving rise to the contained events have energies $E_\nu \leq 1.2$ GeV, with a rapidly falling spectrum. As we shall see, the neutrino-oscillations solution requires the absolute value of the squared mass difference to be always larger than 10^{-3} eV². The maximum density of the earth is $\rho \simeq 12.5$ g cm⁻³, therefore for contained events matter effects are practically negligible.

Matter effects are on the contrary significant for upward-going muons, the reason being that the neutrino energies involved are one to two orders of magnitude larger than those for contained events.

The matter effects on the oscillations of neutrinos responsible for the upward-going muons have been considered in²¹. The results for the $\nu_\mu \leftrightarrow \nu_\tau$ and $\nu_\mu \leftrightarrow \nu_s$ oscillations, along with the constraints from the other experiments, are summarized in fig. 1. In this figure three limiting curves are the results of experiments that do *not* involve upward-going muons. Curve (a) is obtained from accelerator experiments²² and the allowed region is below the curve. Curve (b) is obtained from the result of Fréjus¹¹ on the e/μ ratio of contained events; this result is consistent with the no-oscillation hypothesis, and the allowed region is to the left of the curve. Curve (c) is obtained from the observation of an anomaly in the same e/μ ratio by Kamiokande and IMB^{1,3}; this is a “positive result” and the allowed region is to the right of the curve. These three limits apply equally to the $\nu_\mu \leftrightarrow \nu_\tau$ and $\nu_\mu \leftrightarrow \nu_s$ oscillations which differ from each other only because of the matter effects. These effects are obviously irrelevant to the accelerator limit, and almost so also for (b) and (c) curves, although approximately half of the contained events observed in IMB and Kamiokande are produced by neutrinos that have penetrated through the earth. This fact has already been explained above (see the discussion after Eq. 5).

The limits obtained from the total flux of upward-going muons using the criterion²¹

$$F \leq 0.75 F_0, \quad (6)$$

F_0 being the average flux calculated in the absence of the oscillations, are shown in fig. 1 by the curves A_τ , A_{s+} and A_{s-} , the subscript indicating the flavour of the neutrino mixed with the ν_τ . The case ν_s is described by two curves because one needs to consider the sign of Δm^2 whenever the matter effects on neutrino oscillations are important.

The limits obtained from the stopping/passing ratio using the criterion²¹

$$\frac{F_s}{F_p} \leq 0.8 \left(\frac{F_s}{F_p} \right)_0, \quad (7)$$

where the subscript “0” stands for the ratio of fluxes in the absence of the oscillations, are shown in the same figure by the curves B_τ , B_{s+} and B_{s-} .

Comparing the three type *A* curves we can make the following observations. When $\Delta m^2 < 0$ ($\Delta m^2 > 0$) for oscillations of neutrinos (antineutrinos) the MSW resonant enhancement²⁰ will occur. Since ν_μ 's are more abundant (and have a larger cross section) than $\bar{\nu}_\mu$'s, the same values of $\sin^2 2\theta$ and $|\Delta m^2|$ will result in a stronger suppression of the upward-going muon flux if Δm^2 is negative and the MSW resonance is relevant for neutrinos. For $|\Delta m^2| \gtrsim 1 \text{ eV}^2$ the three curves A_τ , A_{s+} and A_{s-} almost coincide; this is a reflection of the fact that for large $|\Delta m^2|/E$ matter effects are not significant.

Very similar considerations can be made about the curves B_τ , B_{s+} and B_{s-} . For maximal mixing, the region of $|\Delta m^2|$ that can be excluded in the case of $\nu_\mu \leftrightarrow \nu_s$ oscillations is moved to values of $|\Delta m^2|$ larger by a factor 2.8 than in the $\nu_\mu \leftrightarrow \nu_\tau$ case. For oscillations into sterile neutrinos, when the mixing is smaller than unity, the limit that applies for

$\Delta m^2 < 0$ is stronger than for the other case. This is again because when the MSW resonance occurs for neutrinos (antineutrinos) the sensitivity to the oscillations is stronger (weaker). A detailed analysis must also take into account the fact that when the neutrinos go through the oscillation resonance the oscillation length passes through a maximum. This is the reason why the limit B_{s+} is stronger than the limit B_{s-} in a limited region of parameter space. For maximal mixing the curves B_{s+} and B_{s-} end in the same points.

The most significant difference between the limits for the $\nu_\mu \leftrightarrow \nu_\tau$ and $\nu_\mu \leftrightarrow \nu_s$ oscillations is in the region of low squared mass differences. A region of the parameter space $|\Delta m^2| = (3 \div 7) \times 10^{-4} \text{ eV}^2$ and $\sin^2 2\theta \geq 0.7$ is excluded for the ν_τ but not for ν_s oscillations. This region is however already excluded by curve (c), provided that the anomaly in the e/μ ratio of contained events is due to neutrino oscillations. As shown in fig. 1, for both types of oscillations there is a region of parameter space which is compatible with all existing experimental measurements. The range of allowed values for the parameters is in both cases roughly: $0.4 \lesssim \sin^2 2\theta \lesssim 0.7$ and $2 \times 10^{-3} \text{ (eV}^2) \lesssim |\Delta m^2| \lesssim 0.4 \text{ (eV}^2)$. The allowed region for ν_s is somewhat smaller but contains also a small part (for large positive Δm^2) which is not allowed for ν_τ . In future, with more data, the sensitivity of the curves of type B (which is determined by the statistical errors) will improve, exploring the low $|\Delta m^2|$ part of the allowed region. To improve the sensitivity of the curves of type A , one needs rather to reduce the theoretical systematic uncertainties. If these could be reduced to the level of 15% (at 90% c.l.) the entire allowed region of parameter space would then be explored by measurements of upward-going muons and one would be able to either confirm or disprove the neutrino oscillations as a solution to the atmospheric neutrino puzzle.

As we have seen, the oscillations of ν_μ into a sterile neutrino state ν_s can be strongly affected by the matter of the earth. One should notice that although the existence of a sterile neutrino does not contradict any laboratory data, it can be in conflict with cosmological considerations. Namely, for large enough values of the mixing angle and Δm^2 , $\nu_\mu \leftrightarrow \nu_s$ oscillations can bring the sterile neutrinos into equilibrium with matter before the nucleosynthesis epoch thereby affecting the primordial ${}^4\text{He}$ abundance in the universe. The analysis sets the maximum allowed number of “light neutrinos” N_ν to 3.4. In order not have $N_\nu > 3.4$ for oscillations between sterile and muon neutrinos one needs $\Delta m^2 < 8 \times 10^{-6} \text{ eV}^2$ for maximal mixing (see²³ for more details). Clearly, with the values $|\Delta m^2| > 2 \times 10^{-3} \text{ eV}^2$ this bound would be violated, and one would have $N_\nu = 4$.

The situation about the experimentally allowed values of the oscillation parameters in the case of the $\nu_\mu \leftrightarrow \nu_e$ oscillations is summarized in fig. 2. The results from the analysis of solar neutrino experiments refer to lower values of $|\Delta m^2|$ and are not shown. As in fig. 1, three limiting curves are the results of experiments that do *not* involve upward-going muons. Curve (a) is the limit obtained from reactor experiments²⁴, curve (b) and (c) are obtained from measurements of the e/μ ratio of contained events in the Fréjus¹¹ and Kamiokande and IMB experiments^{1,3}. As before, curve (b) excludes the region to its right, curve (c) the region to its left.

The limits obtained from the measurement of the total upward-going muon flux according to the criterion of Eq. 6 is shown by curves A_{e+} and A_{e-} , the two curves referring to the sign of Δm^2 as before. The region excluded by the curves of type A is well inside

the region of parameter space already excluded by the Gösgen reactor experiment. Matter suppresses the oscillations more strongly than in the $\nu_\mu \leftrightarrow \nu_s$ case, since the difference in the effective potentials is twice as large now²¹. One also has to take into account the fact that in cosmic ray showers a $\nu_e(\bar{\nu}_e)$ flux is produced as well. Both effects reduce the sensitivity of the measurement to the $\nu_\mu \leftrightarrow \nu_e$ oscillations.

For the $\nu_\mu \leftrightarrow \nu_e$ oscillations, the condition of Eq. 7 is never satisfied²¹ and therefore no limit can be obtained from the stopping/passing ratio. In the case of maximal mixing, F_s/F_p reaches (for $|\Delta m^2| = 6 \times 10^{-2} \text{ eV}^2$) a minimum value of 0.150, only 19% smaller than the value calculated in the absence of oscillations. Curves B_{e+} and B_{e-} are calculated with the more demanding criterion $F_s/F_p \leq 0.9 (F_s/F_p)_0$. They are an indication of the sensitivity that could be obtained with a sample of data approximately four times the one collected by IMB.

As shown in fig. 2, a small region of parameter space $0.35 \lesssim \sin^2 2\theta \lesssim 0.7$ and $4 \times 10^{-3} \text{ (eV}^2) \lesssim |\Delta m^2| \lesssim 2 \times 10^{-2} \text{ (eV}^2)$ is compatible with all existing experimental measurements.

As we have seen the complex of data induced by atmospheric neutrinos (contained and upward-going muons) may be described in terms of neutrino oscillations. The matter effects are important in the precise determination of the allowed parameter region.

Proton decay

Another possible explanation of the anomaly observed in the contained events in underground detectors is the decay²⁵

$$p \rightarrow e^+ + \nu_e + \bar{\nu}_e. \quad (8)$$

Such a decay would produce an excess of electron neutrinos. Obviously, the decay neutrinos would have the energy $< 1 \text{ GeV}$ and so the data on the upward-going muons would not be affected. The contained data can be accounted for provided the proton lifetime with respect to the process (8) is $\tau_p = (3.7_{-1.0}^{+1.9}) \times 10^{31} \text{ yr}$. One should keep in mind that although the existing lower limits on the proton lifetime seem to exclude such short a lifetime, these limits actually do not apply to the exotic decay mode of Eq. 8, and so the proton decay is still a viable explanation of the atmospheric neutrino anomaly. This possibility can be checked experimentally. The Soudan 2 detector is capable of detecting the proton recoil in the process

$$\nu_e + N \rightarrow e^- + p. \quad (9)$$

If the proton decay hypothesis is correct, a fraction of the electron-like events should be due to the decay (8), and not to the reaction (9); thus one should see fewer recoil protons than expected in the electron-like events¹³. So far, Soudan 2 have not seen any deficiency of recoil protons in their data. New data with higher statistics will probably shed some light on this exciting possibility.

4 Summary and outlook

The contained event data in the underground water Čerenkov detectors shows a reduced (μ/e) ratio implying a deficiency of atmospheric ν_μ 's or an excess of ν_μ 's. The results of iron calorimeters are consistent with both the reduced and unsuppressed (μ/e) ratio because of their statistics being too low.

Possible explanations of the observed anomaly include neutrino oscillation and proton decay. All kinds of neutrino oscillations ($\nu_\mu \leftrightarrow \nu_\tau$, $\nu_\mu \leftrightarrow \nu_e$, $\nu_\mu \leftrightarrow \nu_s$) can account for the atmospheric neutrino anomaly. The data on upward going muons severely constrain the allowed ($\Delta m^2, \sin^2 2\theta$) space for neutrino oscillations but do not exclude them as a possible solution of the problem. Matter effects on neutrino oscillations are important for the precise determination of the allowed parameter region.

There are a number of theoretical works yielding the neutrino masses and mixings which can simultaneously explain the atmospheric neutrino anomaly and the solar neutrino problem through the (different kinds of the) neutrino oscillations. Upward-going muons data rules out large mixing angles ($\sin^2 2\theta > 0.6-0.8$) in atmospheric neutrino oscillations, thereby severely constraining the theoretical models.

Is the atmospheric neutrino anomaly a manifestation of new physics or an instrumental effect? At present, we don't have a definite answer. Still there are possibilities to improve our understanding of the problem. For the analyses of the data accurate calculations of the atmospheric neutrino fluxes are required. At present the uncertainties in these calculations are rather large. To improve the situation, new measurements of primary cosmic ray spectra and composition would be highly desirable. The neutrino-nucleus cross sections introduce large uncertainties in the calculated spectra ($\sim 10\%$). More accurate cross sections are needed. For the interpretation of the data of the Čerenkov detectors, the μ/e identification probability is crucial. Although the results obtained with two different identification techniques agree very well with each other, direct check of the μ/e identification probability in water would be welcome. The Kamiokande collaboration is planning to perform the direct experiment using the KEK Proton-Synchrotron with μ , e and π beams with the momenta $p = 200-1000$ MeV/ c . The 1000 t detector is ready, and the experiment was scheduled to start (and probably started) in December 93.

To check the neutrino oscillations hypothesis, direct long-baseline accelerator experiments covering the interesting oscillation parameter range would be of crucial importance. There were several proposals of such experiments, including the Super-Kamiokande and Icarus experiments using the neutrino beams from CERN and the Soudan 2 experiment using the FNAL beam. Recently another experiment, using high intensity neutrino beam of the AGS accelerator of the Brookhaven National Laboratory, has been proposed.

Thus, much work has to be done to clear up the situation with the atmospheric neutrino anomaly.

It is a pleasure to thank Paolo Lipari and Maurizio Lusignoli in collaboration with whom the work²¹ has been done. Useful discussions with Zurab Berezhiani and Alexei Smirnov are gratefully acknowledged.

References

- [1] K.S. Hirata *et al.* (Kam-II Collaboration), *Physics Letters* **B280** (1992) 146.
- [2] A. Suzuki, in *Proc. 5th Int. Workshop on Neutrino Telescopes*, ed. Milla Baldo Ceolin (Padova, 1993), p. 221.
- [3] R. Becker-Szendy *et al.* (IMB Collaboration), *Phys. Rev.* **D46** (1992) 3720. See also D. Casper *et al.*, *Phys. Rev. Lett.* **66** (1991) 2561.
- [4] G. Barr, T.K. Gaisser and T. Stanev, *Phys. Rev.* **D39** (1989) 3532; H. Lee and Y.S. Koh, *Nuovo Cimento* **B105** (1990) 883; M. Honda, K. Kasahara, K. Hidaka and S. Midorikawa, *Phys. Lett.* **B248** (1990) 193; M. Kawasaki and S. Mizuta, *Phys. Rev.* **D43** (1991) 2900; E.V. Bugaev and V.A. Naumov, *Phys. Lett.* **B232** (1989) 391.
- [5] E.W. Beier *et al.*, *Phys. Lett.* **B283** (1992) 446.
- [6] R. Becker-Szendy *et al.* (IMB Collaboration), *Phys. Rev. Lett.* **69** (1992) 1010.
- [7] S.P. Mikheyev, in *Proc. Int. Workshop on ν_μ/ν_e Problem in Atmospheric Neutrinos*, ed. V Berezinsky and G. Fiorentini, (Gran Sasso, L'Aquila, 1993), p. 144.
- [8] M. Mori *et al.* (Kamiokande Collaboration), *Phys. Lett.* **B270** (1991) 89.
- [9] T. Stanev, in *Proc. 5th Int. Workshop on Neutrino Telescopes*, ed. Milla Baldo Ceolin (Padova, 1993), p. 247.
- [10] A. Suzuki, in *Proc. Int. Workshop on ν_μ/ν_e Problem in Atmospheric Neutrinos*, ed. V Berezinsky and G. Fiorentini, (Gran Sasso, L'Aquila, 1993), p. 71.
- [11] Ch. Berger *et al.* (Fréjus Collaboration), *Phys. Lett.* **B245** (1990) 305; **B227** (1989) 489; L. Moscoso, in *Proc. Int. Workshop on ν_μ/ν_e Problem in Atmospheric Neutrinos*, ed. V Berezinsky and G. Fiorentini, (Gran Sasso, L'Aquila, 1993), p. 100.
- [12] M.A. Aglietta *et al.* (NUSEX Collaboration), *Europhys. Lett.* **8** (1991) 611.
- [13] P. Litchfield, in *Proc. Int. Workshop on ν_μ/ν_e Problem in Atmospheric Neutrinos*, ed. V Berezinsky and G. Fiorentini, (Gran Sasso, L'Aquila, 1993), p. 114.
- [14] V. Agraval, T.K. Gaisser and T. Stanev, in preparation.
- [15] A.V. Butkevich, L.G. Dedenko and I.M. Zheleznykh, *Yad. Fiz.* **50** (1989) 142 (*Sov. J. Nucl. Phys.* **50** (1989) 90).
- [16] K. Mitsui, Y. Minorikawa and H. Komori, *Nuovo Cimento* **9C** (1986) 995.
- [17] L.V. Volkova, *Yad. Fiz.* **31** (1980) 784 (*Sov. J. Nucl. Phys.* **31** (1980) 1510).
- [18] J.F. Owens, *Phys. Lett.* **B266** (1991) 126.
- [19] E. Eichten, I. Hinchcliffe, K. Lane and C. Quigg, *Rev. Mod. Phys.* **56** (1984) 579 (Erratum 58 (1986) 1065).

- [20] S.P. Mikheyev, A.Yu. Smirnov, *Yad. Fiz.* **42** (1985) 1441 [*Sov. J. Nucl. Phys.* **42**, 913 (1985)]; L. Wolfenstein, *Phys. Rev.* **D17** (1978) 2369.
- [21] E. Akhmedov, P. Lipari and M. Lusignoli, *Phys. Lett.* **B300** (1993) 128.
- [22] F. Dydak *et al.* (CDHS Collaboration), *Phys. Lett.* **B134** (1984) 281; F. Bergsma *et al.* (CHARM Collaboration), *Phys. Lett.* **B142** (1984) 183.
- [23] K. Enqvist, K. Kainulainen, M. Thomson, *Phys. Lett.* **B288** (1992) 145.
- [24] G. Zacek *et al.*, *Phys. Rev.* **D34** (1986) 2621.
- [25] W.A. Mann, T. Kafka and W. Leeson, *Phys. Lett.* **B291** (1992) 200.

Figure Captions

Fig. 1 Limits for the oscillation parameters Δm^2 and $\sin^2 2\theta$ in the case of $\nu_\mu \leftrightarrow \nu_\tau$ and $\nu_\mu \leftrightarrow \nu_s$ mixing. The curves A_τ , A_{s^+} and A_{s^-} are limits obtained from the measurements of the total flux of upward-going muons. The curves B_τ , B_{s^+} and B_{s^-} are obtained from the measurements of the stopping/passing ratio. Also plotted are the 90% c.l. limits from accelerator experiments (a), and the from the measurement of the e/μ ratio of contained events in the Fréjus (b) and Kamiokande experiments (c).

Fig. 2. Limits for the oscillation parameters Δm^2 and $\sin^2 2\theta$ in the case of $\nu_\mu \leftrightarrow \nu_e$ mixing. The curves A_{e^+} and A_{e^-} are obtained from the measurements of the total flux of upward-going muons. The curves B_{e^+} and B_{e^-} are in this case estimates of the sensitivity of future measurements of the stopping/passing ratio (see text). Also plotted are the 90% c.l. limits from the Gösgen reactor experiment (a), and from the e/μ ratio of contained events in Fréjus (b), and Kamiokande (c).

This figure "fig1-1.png" is available in "png" format from:

<http://arxiv.org/ps/hep-ph/9402297v1>

This figure "fig1-2.png" is available in "png" format from:

<http://arxiv.org/ps/hep-ph/9402297v1>